

# Spin Chirality in a Molecular Dysprosium Triangle: the Archetype of the Non-Collinear Ising Model

Javier Luzon,<sup>1</sup> Kevin Bernot,<sup>1</sup> Ian J. Hewitt,<sup>2</sup> Christopher E. Anson,<sup>2</sup> Annie K. Powell,<sup>2</sup> and Roberta Sessoli\*<sup>1</sup>

<sup>1</sup>*Laboratory of Molecular Magnetism, Department of Chemistry and INSTM (UdR Firenze),  
Università degli Studi di Firenze, Via della Lastruccia 3, 50019, Sesto Fiorentino, Italy*

<sup>2</sup>*Institut für Anorganische Chemie, Universität Karlsruhe (TH), Engesserstr. 15, 76131 Karlsruhe, Germany*  
(Dated: April 8, 2008)

Single crystal magnetic studies combined with a theoretical analysis show that cancellation of the magnetic moments in the trinuclear  $\text{Dy}^{3+}$  cluster  $[\text{Dy}_3(\mu_3\text{-OH})_2\text{L}_3\text{Cl}(\text{H}_2\text{O})_5]\text{Cl}_3$ , resulting in a non-magnetic ground doublet, originates from the non-collinearity of the single ion easy axes of magnetization of the  $\text{Dy}^{3+}$  ions that lie in the plane of the triangle at  $120^\circ$  one from each other. This gives rise to a peculiar chiral nature of the ground non-magnetic doublet and to slow relaxation of the magnetization with abrupt accelerations at the crossings of the discrete energy levels.

PACS numbers: 71.79.Ej, 75.10.Jm, 75.50.Xx, 75.30.Cr

Molecular nanomagnetism has provided benchmark systems to investigate new and fascinating phenomena in magnetism[1, 2] like magnetic memory at the molecular level[3], quantum tunneling of the magnetization[4, 5], or destructive interferences in the tunneling pathways[6]. In this field rare earth ions like dysprosium(III) are currently investigated because of their large magnetic anisotropy and high magnetic moment[7]. In the course of our synthetic efforts to obtain new molecular nanomagnets based on rare-earth ions we recently obtained the trinuclear  $\text{Dy}^{3+}$  cluster  $[\text{Dy}_3(\mu_3\text{-OH})_2\text{L}_3\text{Cl}(\text{H}_2\text{O})_5]\text{Cl}_3$  (where L is the anion of ortho-vanillin)[8], hence abbreviated as  $\text{Dy}_3$ , which possesses an almost trigonal ( $C_{3h}$ ) symmetry (see Figure 1 and EPAPS for more information)[9].

Preliminary powder magnetic measurements measure-

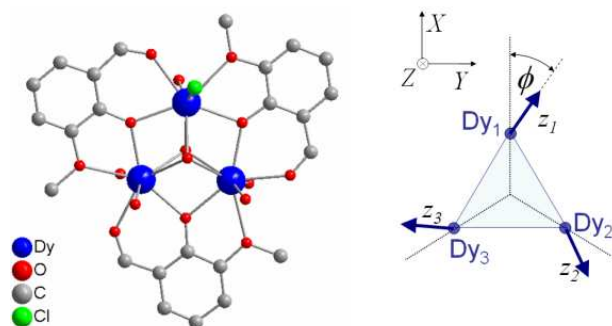


FIG. 1: (color online) Left: View of the molecular structure of  $\text{Dy}_3$  cluster where the hydrogen atoms, the chloride counteranions and the solvent molecules of crystallization have been omitted. Right: Schematic view of the spin structure of the  $\text{Dy}_3$  triangular cluster and of the local easy axes orientation in respect of the laboratory  $XYZ$  reference frame.

ments on two compounds containing such  $\text{Dy}_3$  clusters, but differing in their crystal packing and intermolecular contacts, revealed an identical magnetic behavior where the magnetization vs. field curve at low temperature is almost flat, suggesting a non magnetic ground state, but suddenly increases to its saturation value,  $M_s$ , at  $H = 8$  kOe[8]. This is in contrast to what commonly observed for antiferromagnetic triangular clusters that show a multi-step magnetization curve [10]. A possible explanation is that the  $\text{Dy}^{3+}$  ions are characterized by almost ideal Ising anisotropy with the single ion easy axes lying in the plane of the triangle at  $120^\circ$  from one another, as represented in the scheme of Figure 1. To the best of our knowledge an experimental realization of this simple but fascinating spin structure is unprecedented.

To verify our hypothesis larger crystals (of size *ca.*  $1 \text{ mm}^3$ ) of one of the two compounds were grown according to [8] through very slow evaporation of the solvent. This allowed an accurate face indexing of the crystal on the X-ray diffractometer and the investigation of the magnetic anisotropy by using an horizontal sample rotator in the SQUID magnetometer (see EPAPS for experimental details)[9]. Scans in different crystallographic planes allowed us to determine the three magnetic anisotropy axes, denoted as  $X$ ,  $Y$  and  $Z$ . The two structurally equivalent  $\text{Dy}_3$  molecules in the unit cell have the  $\text{Dy}_3$  planes almost perpendicular to  $Z$  and one side of the triangle parallel to  $Y$  (see Fig. 1). Magnetization vs. field curves along these axes are given in Figure 2a. Along  $X$  and  $Y$  a sudden jump around 8 kOe is observed while an almost linear but weaker magnetization is observed along  $Z$ . In Figure 2b the temperature dependence of the magnetization along the three axes measured at 1 kOe, and thus before the jump to saturation, are shown. The in-plane  $X$  and  $Y$  directions are very similar and  $M$  tends to zero at low temperatures, confirming a non-magnetic ground state, while a weaker signal is observed along  $Z$ .

\*corresponding author: roberta.sessoli@unifi.it

The observed behaviour has been modelled using the canonical formalism of the statistical thermodynamics

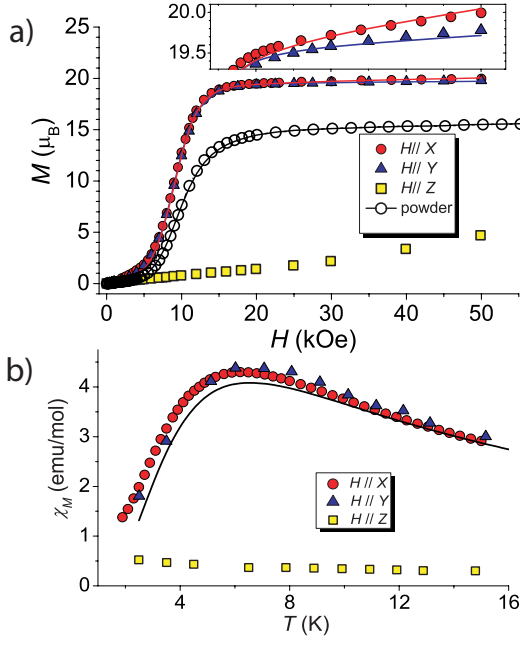


FIG. 2: (color online) a) Field dependence of the magnetization measured along the X, Y, and Z axes at  $T=1.9$  K. In the inset a magnified view of the high field region is reported. b) Temperature dependence for the susceptibility along X, Y, and Z axes with an applied field of 1 kOe. The solid lines represent the calculated value with Eq. (2) and the best fit parameters discussed in the text.

and taking into account that  $\text{Dy}^{3+}$  ions have a very large magnetic single-ion anisotropy due to the crystal field splitting of the  ${}^6H_{15/2}$  ground state. In a first approximation each  $\text{Dy}^{3+}$  ion, which is supposed to have the doublet ground state well separated in energy from the other excited Stark sublevels, can be represented by an effective spin  $S = 1/2$  and the  $\text{Dy}_3$  system can be modelled by an Ising Hamiltonian:

$$H = - \sum_{i,k=1,2,3}^{i>k} j_{zz} S_{z_i} S_{z_k} - \mu_B \sum_{i=1,2,3} g_z H_z S_{z_i} \quad (1)$$

where for each  $\text{Dy}^{3+}$  ion the  $z_i$  local axis is considered to be in the plane of the triangle at  $120^\circ$  one from each other as schematized in Figure 1. The basis set of the full system consists therefore of 8 vectors:  $|\uparrow\uparrow\uparrow\rangle$ ,  $|\uparrow\uparrow\downarrow\rangle$ ,  $|\uparrow\downarrow\uparrow\rangle$ ,  $|\uparrow\downarrow\downarrow\rangle$ ,  $|\downarrow\uparrow\uparrow\rangle$ ,  $|\downarrow\uparrow\downarrow\rangle$ ,  $|\downarrow\downarrow\uparrow\rangle$ ,  $|\downarrow\downarrow\downarrow\rangle$ , where, however, up and down refers to the local  $z$  axes. Actually, these vectors are already the eigenvectors of (1). The best-fit parameters of the power data were  $j_{zz}/k_B = 10.6(4)\text{K}$  and  $g_z = 20.7(1)$ . This last value confirms that the ground doublet for the  $\text{Dy}^{3+}$  ions is well described by  $|J = 15/2, m_J = \pm 15/2\rangle$ . In fact  $J = 15/2$  results from the coupling of  $L = 5$  and  $S = 5/2$  and thus  $g_J = 4/3$ , which, for  $m_J = \pm 15/2$ , gives an effective gyromagnetic factor of 20.

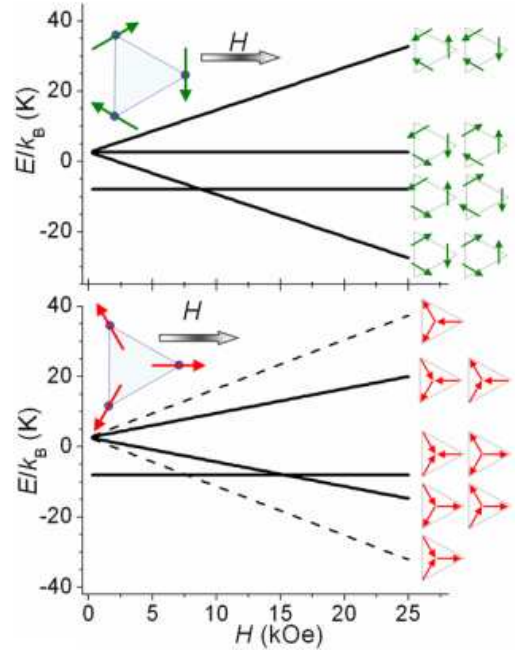


FIG. 3: (color online) a) Zeeman splitting of the levels due to the application of the field along the X axis (bisector) calculated with the Spin Hamiltonian (1) and the parameters indicated in the text, assuming  $\phi = 90^\circ$ . b) Same diagram calculated with  $\phi = 0^\circ$ . The spin structure for each state is schematized by the arrows. The non-degenerate states are highlighted by dash lines.

It is interesting to focus on the energy of the eight eigenstates of the Hamiltonian (1) as a function of the applied magnetic field in the  $\text{Dy}_3$  plane, as shown in Figure 3. At zero field two states with a zero net magnetic moment, are degenerate with energy equal to  $-3j_{zz}/4$ , whereas the other 6 states are also degenerate with energy equal to  $j_{zz}/4$ . In an applied magnetic field the energy of the last six levels depends on the angle the magnetic field forms with the local easy  $z$  axes. Let us suppose that the field is applied along one bisector of the triangle as shown in Figure 3. Two limiting scenarios can be observed depending if the local easy axes are along the edges of the triangle (Fig. 3a) or along the bisectors (Fig. 3b). A jump to saturation magnetization at the first level crossing,  $H_1$ , is expected in both cases, as indeed observed in  $\text{Dy}_3$ . In general, thanks to the structural non-collinearity of the easy axes, the two states of the ground doublet have opposite vortex chirality, with clockwise or anti-clockwise rotation of the spins.

This simple model cannot however reproduce the weak linear increase in the magnetization above the step, visible in the inset of Figure 2a. We have therefore formulated a new Hamiltonian model by considering for each  $\text{Dy}^{3+}$  that the ground state doublet is  $|J = 15/2, m_J = \pm 15/2\rangle$  and that the first excited doublet is  $|J = 15/2, m_J = \pm 13/2\rangle$ . These states can be efficiently admixed by the  $J_+$  and  $J_-$  operators of the Zee-

man interaction. To avoid over-parameterization we have limited the treatment to the first excited doublet. The expression for the new Hamiltonian is:

$$H = -j \sum_{\alpha_i, \alpha_k}^{i,k=1,2,3; i>k} \cos(\hat{\alpha}_i, \hat{\alpha}_k) - g\mu_B \sum_{\alpha_i}^i H_{\alpha_i} S_{\alpha_i} + \frac{\delta}{14} \sum_i ((\frac{15}{2})^2 - S_{z_i}^2) \quad (2)$$

where  $\alpha_i$  runs over the local axes of the  $i$  Dy ion ( $\alpha_i = x_i, y_i, z_i$ ). The first term of (2) comes from considering an isotropic (Heisenberg) exchange between two Dy ions, where  $(\hat{\alpha}_i, \hat{\alpha}_k)$  is the angle between the  $\alpha_i$  and  $\alpha_k$  local axes. The last term describes the single-ion anisotropy and  $\delta$  is the zero field splitting between  $|J = 15/2, m_J = \pm 15/2\rangle$  and  $|J = 15/2, m_J = \pm 13/2\rangle$  states of each  $\text{Dy}^{3+}$  ion. The best fit, again performed on the powder data, provided  $j = -0.092(2)K$ ,  $g = 1.35(1)$  and  $\delta = 102(5)K$ . The  $g$  value is now close to  $4/3$  as expected for  $J = 15/2$ . The large separation between the two Kramers doublets is in good agreement with what is reported in the literature for  $\text{Dy}^{3+}$ [11, 12]. To reproduce the single crystal data the angle  $\phi$  between the  $X$  axis and the local  $z$  anisotropy was allowed to vary freely. The best simulation is obtained with the angles  $\phi = \pm 17(1)^\circ \pm n60^\circ$  ( $n=0,1,2 \dots$ ), where the periodicity results from the symmetry of the cluster. We have also evaluated the intra-molecular dipolar contribution to  $j$  as a function of  $\phi$ , and in the most favourable configuration ( $\phi = 90^\circ$ ) it can only account for about half of the observed value.

Susceptibility measurements using standard induction coils in alternating magnetic field allowed us to estimate the relaxation rate from the frequency dependence of the imaginary component of the susceptibility  $\chi''$  assuming that, according to the Debye model, at the maximum of  $\chi''$  vs  $\omega$  curve the simple relation  $\tau = 1/\omega$  is valid (see EPAPS for more details)[9]. When the  $ac$  field is applied in the plane of the triangle the relaxation rate decreases on lowering the temperature following an Arrhenius law,  $\tau = \tau_0 \exp(\Delta/k_B T)$ , with  $\tau_0 = 2.5(5) \times 10^{-7}$  and  $\Delta = 36(2)$  K. At temperatures below *ca.* 7 K the relaxation increases less rapidly, as shown in Figure 4.

The Arrhenius behavior of the relaxation time characterizes a class of molecular materials called Single Molecule Magnets, SMMs[13], where the easy axis magnetic anisotropy generates a barrier for the reversal of the magnetization giving rise at low temperature to magnetic bistability and memory effect of pure molecular origin[1, 2, 3].  $\text{Dy}_3$ , however, represents the first example where such a slowing down of the magnetization dynamics occurs even if the overall magnetization lies in an almost isotropic plane rather than along an easy axis. That is because the system can be better schematized by three interacting SMMs. In the past pairs of weakly coupled  $\text{Mn}_4$  clusters have been widely investigated[14, 15] and demonstrated to show quantum coherence[16]. However a fascinating new situation is observed in  $\text{Dy}_3$  because the two states of the ground doublet are distinguished by a different spin chirality and they cannot be related

one to each other by a simple exchange of the magnetic sites. The last is verified even in the special non-chiral case of  $\phi = 0^\circ$ .

One of the striking aspect of SMMs is that relaxation at low temperature can occur through an under-

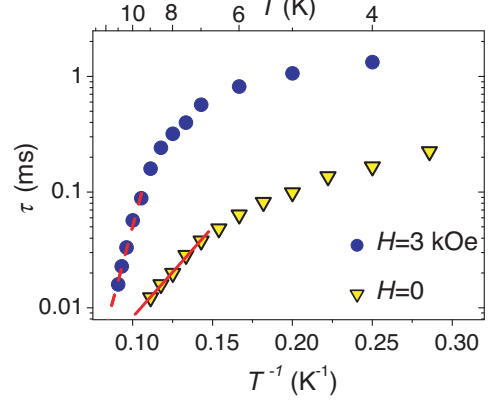


FIG. 4: (color online) Arrhenius plot of the temperature dependence of the relaxation time obtained from the frequency dependence of the  $ac$  magnetic susceptibility in zero and applied static field far from a level crossing. The lines represent the linear fit according to the Arrhenius law of the highest temperature data.

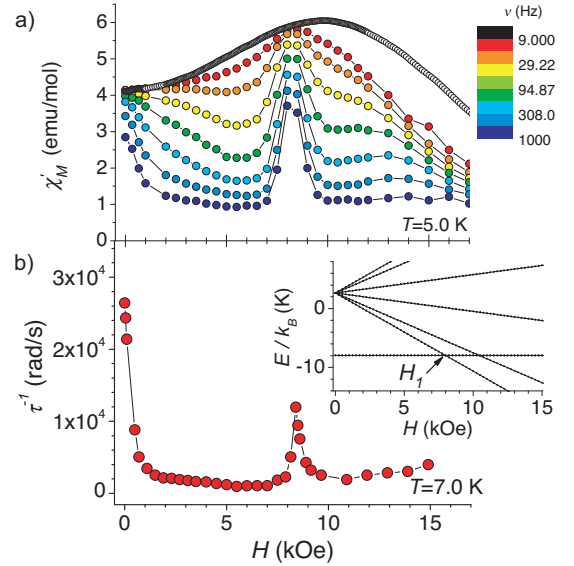


FIG. 5: (color online) a) Field dependence of the real component at 5 K of the  $ac$  susceptibility measured with the field along  $X$  at logarithmic spaced frequencies. The empty circles represent the experimental static susceptibility obtained by derivation of the experimental magnetization curve. b) Field dependence of the relaxation time measured at  $T=7$  K with the field applied along  $Y$ . In the inset the Zeeman splitting calculated for  $H$  parallel to  $Y$  with the best fit parameters discussed in the text.

barrier mechanism[1]. The tunneling is particularly efficient close to zero field, where the maximum degeneracy of the states is observed[4, 5]. The application of a static field has indeed a strong influence on the dynamics of the magnetization of  $\text{Dy}_3$ , as shown in Fig. 5a where the real component of the susceptibility,  $\chi'$ , for different frequencies in 1-1000 Hz range is shown as a function of the field. Around zero field and the first level crossing,  $H_1$ , the dynamic susceptibility approaches the equilibrium value, i.e. that obtained from the derivative of the static magnetization curve recorded at the same temperature, while for intermediate fields a strong frequency dependent reduction, arising from the impossibility to follow the oscillating field, is observed. Similar results have been obtained along  $Y$ , as shown in Fig 5b where the field dependence of the relaxation rate at  $T=7$  K for this orientation is given. The acceleration of the relaxation occurs at a field slightly smaller than that corresponding to the maximum of the static susceptibility, suggesting that only the first crossing is relevant for the dynamics (inset of Figure 5b). Far from the level crossings, i. e. at  $H=3$  kOe, the relaxation times, given in Fig 4, show a significant increase of the barrier to  $\Delta=120(4)$  K.

The present results are well rationalized by the model we have previously developed. The response in the  $ac$  field mainly involves transfer of the population from/to the ground doublet to/from the first magnetic excited state, implying the reversal of one spin inside the triangle. Far from any level crossings this seems to occur through an Orbach process involving the first excited Kramers doublet of each of the  $\text{Dy}^{3+}$  ions, and its energy gap  $\delta$ , estimated from the static properties, is found indeed to be in good agreement with the observed activation energy  $\Delta$ . On the contrary, at  $H=0$  the reduction of the barrier

suggests that an alternative mechanism takes place. Tunneling of the magnetization has already been observed for other lanthanide-based SMM and is attributed to the admixture in zero external field of the ground Kramers doublet states, made possible by the hyperfine interaction [17, 18]. At the first level crossing the situation of zero local field is reestablished for a  $\text{Dy}^{3+}$  ion resulting in the observed fast dynamics.

To conclude,  $\text{Dy}_3$  has revealed to be a benchmark system to investigate non-collinearity in Ising systems. It is worth stressing that non-collinearity is a key feature of molecular magnetism, where complex building-blocks characterized by low symmetry are assembled in more symmetric architectures.  $\text{Dy}_3$  combines the slow dynamics of Single Molecule Magnets and the level crossing observed in antiferromagnetic rings[19, 20]. Both types of systems are currently being investigated for their potential application in quantum computation[21, 22, 23, 24] and systems with a non-magnetic nature of the ground doublet state could be used in order to reduce decoherence effects due to the fluctuation of local magnetic fields. In the ideal case when the spins lie exactly on the plane of the triangle the dynamics involving the ground doublet is however not directly accessible with magnetometry and requires to be further investigated with more sophisticated techniques, for instance using local probes like muons or neutrons.

We acknowledge financial support from the NE-MAGMANET (FP6-NMP3-CT-2005-515767) and the German DFG (SPP1137 and the Center for Functional Nanostructures, CFN). W. Wernsdorfer, A. Vindigni, D. Gatteschi, and M. G. Pini are gratefully acknowledged for stimulating discussion and helpful suggestions.

- 
- [1] D. Gatteschi, R. Sessoli, and J. Villain, *Molecular nanomagnets* (Oxford University Press, Oxford, 2006).
  - [2] G. Christou, *Polyhedron* **24**, 2065 (2005).
  - [3] R. Sessoli, D. Gatteschi, A. Caneschi, and M. Novak, *Nature* **365**, 141 (1993).
  - [4] J.R. Friedman, M.P. Sarachik, J. Tejada, and R. Ziolo, *Phys. Rev. Lett.* **76**, 3830 (1996).
  - [5] L. Thomas *et al.*, *Nature* **383**, 145 (1996).
  - [6] W. Wernsdorfer and R. Sessoli, *Science* **284**, 133 (1999).
  - [7] N. Ishikawa, M. Sugita, T. Ishikawa, S. Koshihara, and Y. Kaizu, *J. Am. Chem. Soc.* **125**, 8694 (2003).
  - [8] J. Tang *et al.*, *Angew. Chem. Int. Ed.* **45**, 1729 (2006).
  - [9] See EPAPS Document No. [xxx] for more details of the crystal structure, angle resolved single crystal magnetic measurements, and single crystal alternating current susceptibility measurements. For more information on EPAPS, see <http://www.aip.org/pubservs/epaps.html>.
  - [10] M. Luban *et al.*, *Phys. Rev. B* **66**, 054407 (2002).
  - [11] N. Ishikawa *et al.*, *Inorg. Chem.* **42**, 2440 (2003).
  - [12] C. Benelli and D. Gatteschi, *Chem. Rev.* **102**, 2369 (2002).
  - [13] H. Eppley *et al.*, *Mol. Cryst. Liq. Cryst. Sci. Technol. A* **305**, 167 (1997).
  - [14] W. Wernsdorfer, N. Allaga-Alcalde, D. Hendrickson, and G. Christou, *Nature* **416**, 406 (2002).
  - [15] S. Hill, R. Edwards, N. Aliaga-Alcalde, and G. Christou, *Science* **302**, 1015 (2003).
  - [16] R. Tiron, W. Wernsdorfer, D. Foguet-Albiol, N. Aliaga-Alcalde, and G. Christou, *Phys. Rev. Lett.* **91**, 227203 (2003).
  - [17] R. Giraud, W. Wernsdorfer, A.M. Tkachuk, D. Mailly, and B. Barbara, *Phys. Rev. Lett.* **87**, 057203 (2001).
  - [18] N. Ishikawa, M. Sugita, and W. Wernsdorfer, *Angew. Chem. Int. Ed.* **44**, 2931 (2005).
  - [19] K. Taft *et al.*, *J. Am. Chem. Soc.* **116**, 823 (1994).
  - [20] B. Normand, X. Wang, X. Zotos, and D. Loss, *Phys. Rev. B* **63**, 184409 (2001).
  - [21] M. Leuenberger and D. Loss, *Nature* **410**, 789 (2001).
  - [22] F. Meier, J. Levy, and D. Loss, *Phys. Rev. B* **68**, 134417 (2003).
  - [23] F. Troiani *et al.*, *Phys. Rev. Lett.* **94**, 207208 (2005).
  - [24] S. Bertaina *et al.*, *Nature Nanotech.* **2**, 39 (2007).